Direct Measurement of Valence-Charge Asymmetry by X-Ray Standing Waves

J. C. Woicik,[1] E. J. Nelson,[2] and P. Pianetta[2]
[1]*National Institute of Standards and Technology, Gaithersburg, Maryland 20899*
[2]*Stanford Synchrotron Radiation Laboratory, Stanford, California 94309*
(Received 16 March 1999)

By monitoring valence-photoelectron emission under condition of strong x-ray Bragg reflection, we have determined that a majority of GaAs valence charge resides on the anion sites of this heteropolar crystal, in quantitative agreement with the GaAs bond polarity as calculated from the Hartree-Fock term values. In contrast, the valence-charge distribution in Ge is found to be symmetric. In both cases, the valence emission is found to be closely coupled to the atomic cores.

PACS numbers: 78.70.Ck, 79.60.Bm

Understanding atomic bonding in a solid or film is a classical problem of solid-state physics. While one of the most important experimental tools for the investigation of crystalline solids has been x-ray diffraction, the study of valence-electronic structure lies at the limit of what x-ray diffraction can probe [1].

The difficulty encountered in such x-ray diffraction measurements arises from the fact that all of the electrons within the crystalline-unit cell contribute to the elastic scattering of photons; consequently, the elastic scattering arising from the valence electrons cannot be experimentally discriminated from the elastic scattering arising from the electronic cores. Although detailed valence-charge density maps have been produced by x-ray diffraction for crystals of low atomic number [2], the methodology by which this information is obtained is not straightforward; it relies on the detailed theoretical calculations of the core-electron density that must be utilized in the complex Fourier inversion of the phaseless intensity measurements.

In this Letter, we examine the behavior of the valence-photoelectron emission from two covalently bonded crystals with different degrees of ionicity under the condition of strong x-ray Bragg reflection, i.e., in the presence of the x-ray standing-wave (XSW) interference field generated by the incident and diffracted photon beams. Because we employ an electron analyzer, direct energy discrimination of this inelastic scattering channel is routine for XSW. Additionally, because we track the different electron-emission profiles throughout the entire Bragg-energy gap [3], it will be shown that, due to the physical nature of the photoemission process, the phase of the reflection measured in this way gives a direct, quantitative measure of the bond polarity, i.e., the degree of charge transfer between the atoms involved in the atomic bonding.

The experiment was performed at the Stanford Synchrotron Radiation Laboratory using the "Jumbo" double-crystal monochromator and a standard ultrahigh vacuum chamber. Back-reflection x-ray standing-wave [4] electron-emission patterns were recorded in a fixed-angle, normal-incidence diffraction geometry by scanning the monochromator and a double-pass cylindrical-mirror analyzer (CMA) simultaneously through the photon-energy range of the crystal Bragg back reflection. The CMA was operated with x-ray photoelectron spectroscopy slits and a pass energy of 200 eV to give an electron-energy resolution of ~4 eV. The horizontal axis of the spectrometer was aligned parallel to the polarization vector of the synchrotron radiation, and a pair of InSb(111) crystals provided the monochromatized photon beam. Fiducial information on the photon energy, the photon-energy rocking-curve width (0.7 eV), and control of the sample alignment was obtained from the reflectivity curves which were measured simultaneously to the electron-emission spectra with an I_0 grid upstream of the sample. (111), $(\bar{1}\bar{1}\bar{1})$, and $(-1-1-1)$ x-ray standing-wave data were recorded from freshly cleaved Ge(111), GaAs(110), and GaAs$(-1-10)$ surfaces, respectively. The sample geometry was adjusted to make the incident beam normal to either the (111) or $(-1-1-1)$ diffraction planes.

Figure 1 shows the photoemission spectrum from the Ge(111) surface taken with photon energy $h\nu = 1900$ eV. The emission from the Ge $3d$ core electrons and the crystal-valence band are indicated. The valence emission is composed of the hybridized Ge $4s$ and $4p$ valence states [5].

Figure 2 compares the photon-energy dependence of the Ge $3d$ core-level emission with the Ge valence-electron emission in the vicinity of the Ge(111) Bragg

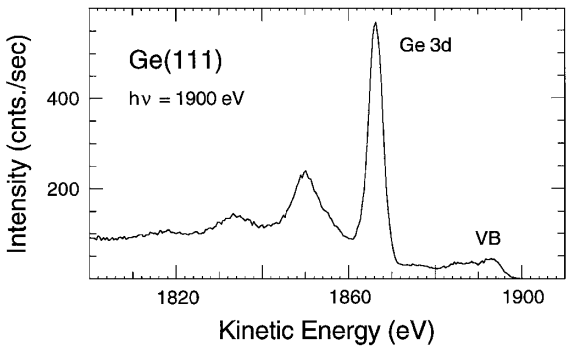

FIG. 1. Photoemission spectrum from crystalline Ge recorded with photon energy $h\nu = 1900$ eV showing the Ge $3d$ and valence-electron emission. The features at lower kinetic energy are the bulk-plasmon losses of the Ge $3d$ core line.

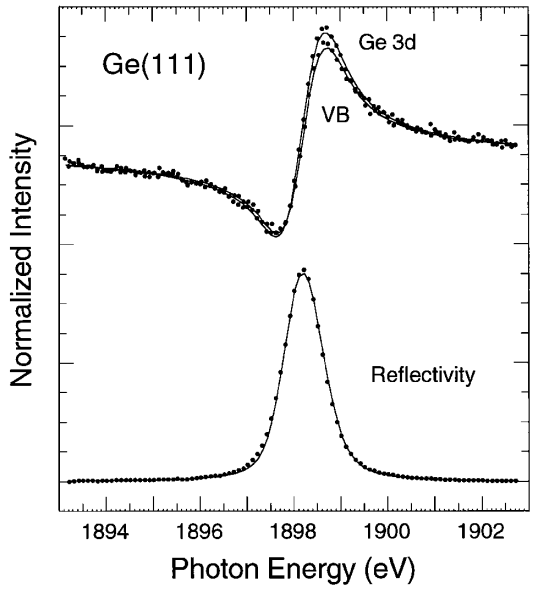

FIG. 2. Photon-energy dependence of the Ge $3d$ and the Ge valence-electron emission near the Ge(111) Bragg back-reflection condition. Also shown is the Ge(111) reflectivity curve. The lines are the theoretical fits to the data points.

back-reflection condition. These are *raw* electron yield curves; they have been scaled only by a constant to make equal their yield away from the energy of the crystal Bragg back reflection. The Ge $3d$ emission shows the characteristic x-ray standing-wave pattern from this centrosymmetric crystal [6]. The valence emission is startlingly similar, showing only a small, but significant reduction in XSW amplitude.

In order to obtain quantitative information, following standard XSW analysis, these data were fit by the function,

$$Y = 1 + R + 2\sqrt{R}\,F\cos(\phi - 2\pi D), \qquad (1)$$

using the photon-energy offset and photon-energy width obtained from the fit to the reflectivity. ϕ is the phase of the standing wave, which is defined through the reflectivity R. R is obtained from the dynamical theory of x-ray diffraction [7]; both R and ϕ are functions of photon energy.

The pertinent XSW fitting parameters are D, the average position of the resulting emission relative to the diffracting planes in units of the reflecting plane spacing, and F, the coherent fraction of emission that arises from D. For tightly bound core electrons, these parameters are closely related to the x-ray structure factor; for an arbitrary distribution of N atoms, D and F may be interpreted as the phase and amplitude of the charge-density Fourier coefficient for the $\vec{H}$ reflection [8]:

$$Fe^{i2\pi D} = (1/N)\sum_{n=1}^{N} e^{i\vec{H}\cdot\vec{r}_n}. \qquad (2)$$

For the Ge $3d$ core distribution, D and F are found to be 0.010 ± 0.010 and 0.69 ± 0.04, respectively [9]. These parameters are indistinguishable from the expected values of $D = 0$ and $F = 0.71$ for the ideal, nonvibrating [10] lattice sites shown in Fig. 3. Note that, for this centrosymmetric reflection, the (111) atomic planes bisect the Ge(111) double layer; consequently, F is not equal to 1, but, rather, it is equal to $\cos(\pi/4) = \sqrt{2}/2 = 0.71$. This reduction in amplitude reflects the spread of positions between the two identical atoms of the diamond-unit cell, which are displaced by a quarter of a (111) lattice constant along the [111] direction.

In contrast to the yield from the Ge $3d$ core level, the signal recorded by monitoring the crystal-valence emission includes components of different origin. First, there is a contribution from the valence-electron density of states that resides close to the atomic cores. Next, there is a delocalized, overlap component that resides between them [11]. Had our data significantly sampled this intramolecular region of bonding-charge density, then the XSW profile would have been dramatically different from the bulk-XSW pattern shown in Fig. 2. In fact, due to the large amount of charge that is amassed between the atoms [12], it was presumed that the amplitude of the valence-emission pattern would be reduced by a considerable fraction relative to the core-emission pattern [13]. Instead, we have determined $D = 0.000 \pm 0.011$ and $F = 0.66 \pm 0.05$ for the valence distribution, which shows only a small reduction in amplitude relative to the core spectrum. Paradoxically, these data demonstrate that little of the valence-electron emission arises from the delocalized bonding region between the cores.

In order to reconcile our intuition with the experimental measurement, it is useful to examine the basic physics of the photoemission process that leads to these emission patterns. From Bethe and Jackiw [14], the differential cross section of the photoelectric effect due to a monochromatic plane wave is

$$\frac{d\sigma}{d\Omega}(\theta,\phi) \propto \left| \int u_f^* e^{i\vec{k}\cdot\vec{r}}\hat{\varepsilon}\cdot\vec{\nabla}\,u_i\,d^3r \right|^2. \qquad (3)$$

θ and ϕ specify the direction of the ejected photoelectron relative to the incident photon-beam electric polarization vector $\hat{\varepsilon}$. u_i is the initial, bound-state wave function of the electron, and u_f is its final, continuum-state wave function. $\vec{k}$ is the wave vector of the incident photon field, which is perpendicular to $\hat{\varepsilon}$. For core states at typical x-ray energies, the product of $\vec{k}\cdot\vec{r}$ is much less than 1

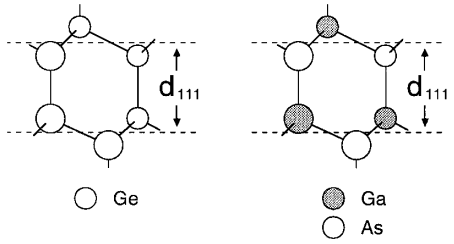

FIG. 3. Side views of the Ge(111) and GaAs(111) crystal structures. The (111) atomic planes are indicated.

whenever u_i gives an appreciable contribution to the integral. Consequently, the spatial part (and more importantly the direction of propagation of the incident and reflected photon beams) of the electric field does not affect the integral; i.e., the electron emission is strictly proportional to the electric-field intensity at the location of the atomic core (dipole approximation), and the standard XSW description [Eq. (1)] applies [15].

Because of the spatial extent of the valence electrons, this situation will not hold for arbitrary photon energy; however, because the valence electrons have negligible binding energy ($\hbar^2 k_f^2/2m = h\nu - \varepsilon_b; \varepsilon_b \sim 0$), the standard XSW description becomes a good approximation at the low x-ray energies. In this case, the final state quickly approaches an energetic plane wave $u_f \sim e^{i\vec{k}_f \cdot \vec{r}}$ (Born approximation), and only the spatial region where u_i is rapidly varying will contribute to the integral. As we know from the success of pseudopotential theory [12], u_i has appreciable high-frequency Fourier components only in the immediate vicinity of the atomic cores. Consequently, it is the localization of the valence emitter for high kinetic-energy photoelectrons [16] that is responsible for the anomalously high, corelike coherent fraction of the valence-XSW pattern shown in Fig. 2.

In a recent study, Solterbeck *et al.* [16] performed a theoretical calculation of the GaAs valence-band density of states and the resulting photon-energy dependence of the photoelectron yield. From an analysis of these calculations, they concluded that for photon energies above 1500 eV the valence emission arises predominantly from a localized region within 0.3 Å of the atomic cores. Using this calculated spread of distances, we may estimate [17] the expected reduction in XSW coherent fraction. The result is ~5%, which is in excellent accord with our experiment.

Having ascertained that the majority of valence-XSW emission arises from a region close to the atomic cores, we may use the bond-orbital approximation [5] and Eq. (2) to construct a model for the valence-XSW emission from the heteropolar GaAs crystal. In the bond-orbital approximation, the expectation value of the electronic position $\vec{r}$ is given by

$$\langle \vec{r} \rangle = \frac{1 + \alpha_p}{2} \vec{r}_a + \frac{1 - \alpha_p}{2} \vec{r}_c . \qquad (4)$$

$\vec{r}_a$ and $\vec{r}_c$ are the atomic coordinates of the As anion and the Ga cation, respectively. α_p is the GaAs bond polarity, which is calculated from the Hartree-Fock term values of the Ga and As atomic $4s$ and $4p$ valence states. Treating the problem within the context of a two-site emitter for this noncentrosymmetric zinc blende structure, Eqs. (2) and (4) lead to the following coherent distance and fraction for the GaAs valence emission relative to the center of the GaAs(111) atomic planes:

$$D = -\frac{1}{2\pi} \tan^{-1}(\alpha_p) \quad \text{and} \quad F = \frac{\sqrt{2}}{2} (1 + \alpha_p^2)^{1/2}. \qquad (5)$$

Using Harrison's [5] theoretical prediction: $\alpha_p = 0.32$, the above equations render $D = -0.049$ and $F = 0.74$.

To test this hypothesis, Fig. 4 shows the GaAs data acquired from the GaAs(111) reflection. Ga $3d$, As $3d$, and the GaAs valence-electron emission patterns were recorded. For the GaAs(111) reflection, the Ga atoms occupy the top half of the diamond bilayer, and the As atoms occupy the bottom half, as shown in Fig. 3. This is easily verified experimentally by the Ga $3d$ and the As $3d$ core-level XSW-emission patterns that show the characteristic yield for each site [6]. These sites are displaced by $+\frac{1}{8}$ (Ga) and $-\frac{1}{8}$ (As) (111) lattice spacings from the center of the GaAs bilayer. The valence spectrum appears similar to the average of the two core-level spectra, but it is shifted significantly towards the As site. Analysis of the valence data produces $D = -0.057 \pm 0.010$ and $F = 0.67 \pm 0.04$. This D coincides with the theoretical prediction based on the bond-orbital model (-0.049), while F shows a similar reduction in amplitude from the ideal-bilayer value as that observed for Ge. (Note that $\alpha_p \equiv 0$ for Ge.)

To demonstrate that this result is not an experimental artifact, we also examined the $(-1\,-1\,-1)$ emission patterns from the same GaAs crystal. These data are shown in Fig. 5. The positions of the Ga and As atoms are now reversed, as seen from the core-level spectra. Once again, the valence emission pattern is close to the average of the two sites, but it is skewed significantly towards the As one. Analysis of the $(-1\,-1\,-1)$ valence data produces $D = +0.068 \pm 0.015$ and $F = 0.60 \pm 0.06$. The center of the $(-1\,-1\,-1)$ valence distribution is equal and opposite (within error) to the center of the (111) valence distribution as necessitated by symmetry; it also shows a

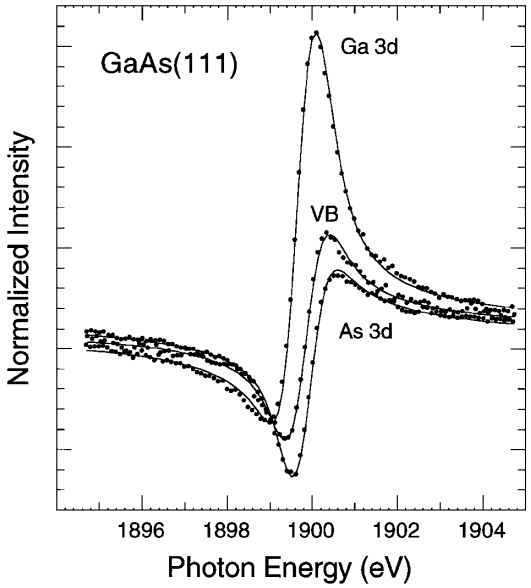

FIG. 4. Photon-energy dependence of the Ga $3d$, the As $3d$, and the GaAs valence-electron emission near the GaAs(111) Bragg back-reflection condition. The lines are the theoretical fits to the data points.

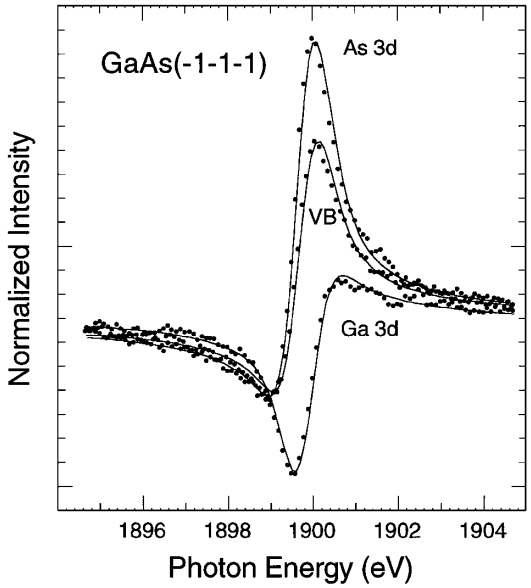

FIG. 5. Photon-energy dependence of the Ga $3d$, the As $3d$, and the GaAs valence-electron emission near the GaAs$(-1\,-1\,-1)$ Bragg back-reflection condition. The lines are the theoretical fits to the data points.

similar reduction in amplitude. Together, the (111) and $(-1\,-1\,-1)$ valence data produce $|D| = 0.060 \pm 0.008$ and $F = 0.65 \pm 0.03$. Because we have measured the coherent position of the valence emission, we may reverse the above formalism to determine α_p directly from the XSW measurement. The result is $\alpha_p = 0.40 \pm 0.06$, which is remarkably close to the theoretical prediction: $\alpha_p = 0.32$ [5].

In conclusion, we have examined the behavior of the valence-photoelectron emission from two covalently bonded crystals under the condition of strong x-ray Bragg reflection. We find that the valence emission arises from a region close to the atomic cores in our x-ray energy range, with little emission emanating from the bonding region between the atoms. We have explained this finding by examining the basic physics of the photoemission process. Additionally, we have found that the valence-charge asymmetry caused by the atomic bonding in a solid may be directly determined by the x-ray standing-wave technique. Our determination of the GaAs bond polarity is in quantitative agreement with the theoretical prediction of the bond-orbital model.

The combination of x-ray diffraction with high-resolution photoelectron spectroscopy should provide an experimental method for obtaining simultaneous energy and position information about the valence-charge distribution in crystalline solids or films. The use of back reflection should allow these measurements to be made on a wide variety of crystalline materials (by relaxing the stringent condition of crystalline perfection), and the measurement of multiple reflections should provide information on the angular distribution of the local bonding.

The authors thank M. H. Chen, B. Crasemann, and W. A. Harrison for useful discussions. This work was performed at the Stanford Synchrotron Radiation Laboratory which is supported by the United States Department of Energy.

[1] C. Kittel, *Introduction to Solid State Physics* (Wiley, New York, 1976), Chap. 2.
[2] G. B. Carpenter, J. Chem. Phys. **32**, 525 (1960); Y. W. Yang and P. Coppens, Solid State Commun. **15**, 1555 (1974).
[3] J. A. Golovchenko, J. R. Patel, D. R. Kaplan, P. L. Cowan, and M. J. Bedzyk, Phys. Rev. Lett. **49**, 560 (1982).
[4] D. P. Woodruff, D. L. Seymour, C. F. McConville, C. E. Riley, M. D. Crapper, N. P. Prince, and R. G. Jones, Surf. Sci. **195**, 237 (1988); J. Zegenhagen, Surf. Sci. Rep. **18**, 199 (1993).
[5] W. A. Harrison, *Electronic Structure and the Properties of Solids* (Freeman, San Francisco, 1980), Chaps. 3 and 7.
[6] J. R. Patel and J. A. Golovchenko, Phys. Rev. Lett. **50**, 1858 (1983).
[7] B. W. Batterman and H. Cole, Rev. Mod. Phys. **36**, 681 (1964).
[8] E. Fontes, J. R. Patel, and F. Comin, Phys. Rev. Lett. **70**, 2790 (1993).
[9] Error bars reflect the spread of values that double the residual chi-squared error.
[10] The inclusion of the Debye-Waller factor would reduce the ideal, bulk coherent fraction from 0.71 to 0.69.
[11] D. R. Jennison, Phys. Rev. Lett. **40**, 807 (1978).
[12] W. A. Harrison, *Solid State Theory* (Dover, New York, 1979), Chaps. 1 and 2.
[13] It is useful to compare the limiting cases: $F = 0$ for a uniform distribution of emission throughout the crystalline-unit cell; $F = 0.5$ for point emitters located at the Ge bond centers; and $F = 0.71$ for point emitters located at the Ge atomic cores.
[14] H. A. Bethe and R. W. Jackiw, *Intermediate Quantum Mechanics* (Benjamin Cummings, Reading, New York, 1986), 3rd ed., Chap. 12.
[15] L. E. Berman and M. J. Bedzyk, Phys. Rev. Lett. **63**, 1172 (1989).
[16] C. Solterbeck, W. Schattke, J.-W. Zahlmann-Nowitzki, K.-U. Gawlik, L. Kipp, M. Skibowski, C. S. Fadley, and M. A. Van Hove, Phys. Rev. Lett. **79**, 4681 (1997).
[17] Assuming uniform emission throughout this region, $\Delta F/F \sim 1 - (2b)^{-1} \int_{-b}^{b} \cos(2\pi x)\, dx$, where $b = 0.3$ Å$/d_{111}$.